ACS APPLIED MATERIALS & INTERFACES

RESEARCH ARTICLE

www.acsami.org

Polymer-Binding Peptides for the Noncovalent Modification of Polymer Surfaces: Effects of Peptide Density on the Subsequent Immobilization of Functional Proteins

Takaaki Date,[†] Jun Sekine,[‡,⊥] Hisao Matsuno,[§,¶] and Takeshi Serizawa*[,†]

[†]Graduate School of Engineering, The University of Tokyo, 7-3-1 Hongo, Bunkyo-ku, Tokyo 113-8654, Japan

[‡]Research Center for Advanced Science and Technology (RCAST), The University of Tokyo, 4-6-1 Komaba, Meguro-ku, Tokyo 153-8904, Japan

[§]Komaba Open Laboratory (KOL), The University of Tokyo, Komaba, Meguro-ku, Tokyo 153-8904, Japan

Supporting Information

ABSTRACT: Peptides that specifically bind to polyetherimide (PEI) were selected, characterized, and used for the noncovalent modification of the PEI surface. The peptides were successfully identified from a phage-displayed peptide library. A chemically-synthesized peptide composed of the Thr-Gly-Ala-Asp-Leu-Asn-Thr sequence showed an extremely high binding constant for the PEI films (5.6×10^8 M^{-1}), which was more than three orders of magnitude greater than that for the reference polystyrene films. The peptide was biotinylated and immobilized onto the PEI films to further immobilize streptavidin (SAv). The amount of SAv bound depended on the density of immobilized peptide. It gradually increased with an increasing density of immobilized peptide and achieved a maximum (2.1 pmol cm^{-2}) at a peptide density of 19.8 pmol cm^{-2}. The ratio of peptide used for immobilizing SAv at the maximum value was only 11%, and was partially due to the low accessibility of SAv to the biotin moieties on the PEI films. Moreover, the amount of SAv bound gradually decreased at higher peptide densities, suggesting that the clustering of the peptides also inhibited the binding of SAv. Furthermore, peptides on the PEI films promoted the uniform immobilization of SAv with less structural denaturing. The immobilized SAv was able to further immobilize probe DNA to hybridize with its complementary DNA. These present results suggest that the density of immobilized peptide has a great impact on the surface modifications using polymer-binding peptides.

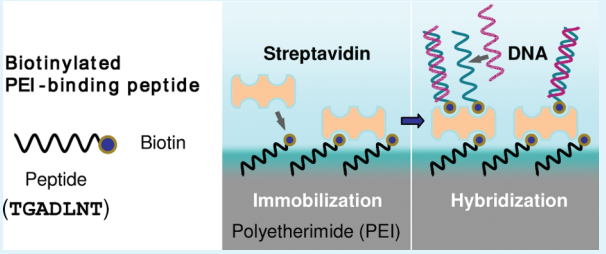

KEYWORDS: material-binding peptide, polyetherimide, surface modification, biotin, streptavidin

INTRODUCTION

Creating the desired interfaces between artificial materials and organisms has become increasingly important in modern science and technology. Several surface modification techniques including covalent and noncovalent methods have been employed. Among these various methods, self-assembled monolayers (SAMs) are often used for surface modifications both practically and experimentally, since they are one of the simplest methods to produce a wide variety of surfaces with well-defined compositions on substrates.[1−3] Many kinds of monolayers can be prepared by changing the adsorbate/substrate combinations, such as fatty acid monolayers on metal oxides,[4,5] organosilicon derivative monolayers on hydroxylated surfaces,[6] organosulfur monolayers on metals,[7] or semiconductors,[8] and alkyl monolayers on hydrogen-terminated silicon.[9] Furthermore, with the development of various kinds of SAMs, biomolecules such as DNA,[10−13] protein,[14−19] and carbohydrate[20−23] were immobilized onto these surfaces to study molecular recognitions. One of the most commonly investigated SAMs is biotin-terminated-SAMs of alkanethiolates on gold to immobilize streptavidin (SAv).[24−29] The biotin-SAv system has expanded the applications of SAMs to study the molecular recognition of biomolecules on material surfaces, and to develop protein chips, protein microarrays, and biosensors. However, most of these studies employ SAMs created on inorganic materials because of the limitations on adsorbate/substrate combinations. If one could extend this to other materials, then it would broaden the range of technical applications and our knowledge of molecular recognition at surfaces.

Material-binding peptides (MBPs) are expected to be a candidate for constructing well-regulated interfaces on the desired materials. In past decades, various inorganic/organic MBPs have been screened from combinatorial peptide libraries displayed on phages and cell surfaces.[30−33] Recent studies have revealed that these MBPs might have specific structures that recognize regularly distributed atoms or functional groups at the material surface, thus leading to specific affinities.[34−41] Notably, a gold-binding peptide

Received: October 9, 2010
Accepted: January 13, 2011
Published: February 2, 2011

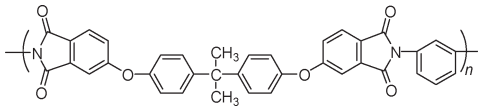

Figure 1. Chemical structure of PEI (Ultem 1000).

was well-characterized, and its adsorption and assembly processes on the Au surface were described in detail,[42] demonstrating that MBPs would be promising tools for constructing material surfaces with desired functions. In fact, many MBPs have already been applied as non-covalently bound linkers for molecular building blocks in nanotechnology such as the attachment of proteins,[43−47] cells,[48−50] inorganic particles,[51−53] and polyethylene glycol.[54,55] Although there are many applications using MBPs as surface modifiers, it still has not been demonstrated in detail that how the peptide density affects the surface modification of materials, which is fundamentally important.

We selected polyetherimide (PEI, Figure 1), an engineering plastic (EP), as a target material for surface modification, considering its biomedical applications. Because of their excellent physico-chemical characteristics, EP-based materials, which are already used widely in advanced industries, have been attractive candidates for replacing metallic materials, and thus have been increasingly employed as biomaterials for trauma, orthopedic, and spinal implants.[56] For this reason, many commercially available EPs such as PEI and polyaryletherketones have been evaluated both in vitro[57−60] and in vivo.[61,62] For example, biocompatibility studies on PEI revealed good cell attachment and growth,[57,59] and a low immune response.[61] Regulating these biological responses as well as adding another function at the EP surface is a key step in successful advanced biomaterials development. For this purpose, several surface modification techniques, such as chemical processes[63−67] and plasma treatments,[68−70] have already been employed. However, these treatments will change the chemical structure of the EP surfaces. There is a growing need for new modification strategies that enable the rapid and easy functionalization of a pristine surface. Thus, identifying EP-binding peptides which may act as linkers for surface modification is important for further applications.

Here, we report the selection and characterization of peptides that specifically bind to PEI, and their applications as surface modifiers. A PEI-binding peptide was identified from a phage-displayed peptide library. Its binding affinity as well as its suitable terminus for introducing a biotin moiety was demonstrated. The biotinylated peptide was immobilized onto PEI films at various densities, and the subsequent immobilization of SAv was evaluated. Furthermore, the immobilized SAv was observed by atomic force microscopy (AFM), structurally analyzed by attenuated total reflection infrared (ATR-IR) spectroscopy, and used for the immobilization of probe DNA to further observe the hybridization with complementary DNA. To our knowledge, this is the first report demonstrating the noncovalent immobilization of functional proteins on polymer surfaces via polymer-binding peptides.

EXPERIMENTAL SECTION

Materials. PEI (Ultem 1000, M_n = 12 000, M_w/M_n = 2.5, GE Plastic) was kindly provided by Fuji Electric Holdings. Polystyrene (PS, M_n = 64 000, M_w/M_n = 1.02) was purchased from Polysciences, and used as the reference polymer. PEI and PS films were prepared by spin-coating from a chloroform solution onto a substrate. Unless otherwise stated, thermally non-treated (as-prepared) films were used. SAv, biotinylated probe DNA (biotin 5′-TAC GCC ACC AGC TCC-3′), and target DNA (5′-GGA GCT GGT GGC GTA-3′) that has a fully complementary sequence to the probe DNA were purchased from Sigma-Aldrich.

Biopanning. Biopanning was performed following a previous report.[38] Briefly, PEI films with a thickness of ∼35 nm were prepared on glass substrates. A 1.2×10^{10} plaque forming unit (pfu)/ 30 μL aliquot of phage library solution (New England Biolabs) in Tris-buffered saline (TBS, 50 mM Tris-HCl, 150 mM NaCl, pH 7.5) was mounted onto the PEI films and incubated for 1 h at ambient temperature. Unbound phages were removed by rinsing the films five times with 150 μL of TBS. The bound phages were eluted by mounting 20 μL of the elution buffer (0.5 M glycine−HCl, 1 mg mL^{-1} bovine serum albumin, pH 2.2) onto the films for 15 min at ambient temperature. The eluted phage solution was neutralized with 7.5 μL of Tris-buffer (1 M Tris-HCl, pH 9.1). The phages were amplified by infecting to *Escherichia coli* strain ER2738, and purified by a polyethylene glycol/NaCl solution to use for the next round of biopanning. Here, four rounds of biopanning were repeated, followed by the cloning and DNA sequencing of the phages.

Phage Binding Analysis. The binding capabilities of the selected phage clones were examined by titer count analysis. A phage solution (30 μL, 500 pM in TBS) was incubated with a PEI pellet, of which the surface area was 35 mm^2, for 1 h at ambient temperature. After rinsing with TBS five times, the bound phages were eluted by 20 μL of the elution buffer for 15 min at ambient temperature. The eluted phage solution was neutralized in the same manner as described above, and the phage amount was determined by titer count analysis, which quantified the number of eluted phages.

Peptide Synthesis. Peptides with a free N terminus and an amidated C terminus were prepared by solid-phase peptide synthesis using standard 9-fluorenylmethyloxycarbonyl (Fmoc)-based procedures as previously reported.[71] The peptide chains were assembled on a NovaSyn TGR resin (amino group 0.22 mmol g^{-1}) using Fmoc amino acid derivatives (3 equiv) in the presence of *N*,*N*-diisopropylethylamine (6 equiv), *O*-benzotriazole-*N*,*N*,*N*′,*N*′-tetramethyl-uronium-hexafluorophosphate (3 equiv), and 1-hydroxybenzotriazole (3 equiv) in a *N*-methylpyrrolidone (NMP)/*N*,*N*-dimethylformamide mixed solvent for coupling, and using 20 % piperidine in NMP for Fmoc group removal. To cleave the peptide from the resin and to remove the side chain protecting groups, the resin was treated with trifluoroacetic acid (TFA)/triisopropylsilane/water (95/2.5/2.5) for 2 h. The mixture was filtered to remove the resin and cooled diethyl ether was added to precipitate the peptide. The precipitate was dried and purified by reverse-phase high-performance liquid chromatography (ELITE LaChrom, HITACHI High-Technologies) using a C18 column (COSMOSIL 5C18-AR-300, 20 × 250 mm, Nacalai Tesque) with a linear gradient of acetonitrile/0.03% TFA at a flow rate of 6 mL min^{-1}. The peptides were identified by matrix-assisted laser desorption ionization time-of-flight mass spectrometry (Autoflex II TOF/TOF, Bruker Daltoniks) using α-cyano-4-hydroxycinnamic acid as a matrix. For the synthesis of biotinylated peptides, the same methodologies were employed using Fmoc-glutamic acid γ-biotinylated through a mono(propylene glycol) and di(ethylene glycol) spacer (*N*-α-Fmoc-*N*-γ-(*N*-biotinyl-3-(2-(2-(3-aminopropyloxy)-ethoxy)-ethoxy)-propyl)-L-glutamine, Supporting Information Figure S1).

SPR Analysis. A Biacore X (GE Healthcare) was used for the SPR analyses, following our previous study.[72] PEI films with a thickness of ∼10 nm were prepared onto gold-coated glass slides (SIA Kit Au, GE Healthcare), and set on the SPR apparatus. HBS-N (10 mM HEPES buffer containing 150 mM NaCl, pH 7.4, GE Healthcare) was flowed at a rate of 20 μL min^{-1} at 25 °C during the experiment. After more than 3 h of HBS-N flow, freshly prepared peptide solutions were applied to the PEI films for 180 sec (association), and then the peptide solutions were exchanged to a peptide-free buffer for 780 sec (dissociation). To evaluate

the slow dissociation precisely, the dissociation time was set longer than in our previous study[72] and baseline corrections (see the Supporting Information for details) were applied. The resulting sensorgrams at 4 concentrations were analyzed by global fitting using BIAevaluation software version 4.1. This program simultaneously fits all sensorgrams, including association/dissociation processes and responses due to rapid changes in the bulk refractive indices when the association/dissociation of the peptide starts, and estimates the association (k_1) (M^{-1} s^{-1}) and dissociation (k_{-1}) (s^{-1}) rate constants. The binding constant (K_a) (M^{-1}) was calculated by $K_a = k_1/k_{-1}$. The fitting results evaluated by the chi-square value (an index of fitting reliability) and standard errors of k_1 and k_{-1} are summarized in Supporting Information Tables S1 and S2. All the chi-square values were less than 9.8, indicating satisfactory evaluation of the peptide binding. Values of less than 10 are considered to be acceptable according to the BIAevaluation handbook. Standard errors were small enough to discuss the values obtained.

For the immobilization of SAv, biotinylated PEI-binding peptides were immobilized onto PEI films, and then after 5 min of HBS-N flow, the SAv solution (250 nM in HBS-N) was applied for 2 min at a flow rate of 5 μL min^{-1} at 25 °C. After the SAv immobilization, probe DNA immobilization (1 μM in HBS-N, 2 min) and target DNA hybridization (1 μM in HBS-N, 5 min) were performed.

Film Characterization. The fluorescence spectra of PEI films (~10 nm thick) on slide glass (Matsunami Glass) were excited at 350 nm and recorded on a spectrofluorometer (FP-6500, Jasco). The slit width was set to 5 nm for both excitation and emission. The static contact angle of the PEI films (~10 nm thick) on Si wafers (0.60−0.65 mm thickness, Sumco) was measured in water with a commercial apparatus (CA-X, Kyowa Interface Science). After the PEI films were conditioned in water or in a peptide solution, 3 μL of sessile air bubbles were attached to the underside of the PEI films in water using a microsyringe. The bubble shapes were captured by monitor and the contact angles were calculated. The topologies of the PEI films were visualized by non-contact mode AFM (SPM-9600, Shimadzu) in air using a silicon cantilever (PointProbe, NCH, resonance frequency 320 kHz, force constant 42 N m^{-1}, NanoWorld). The changes in the film thickness of the PEI films were measured by scratching-mode AFM (SPM-9600, Shimadzu) in air and in HBS-N using a silicon nitride cantilever (OMCL-TR800PSA-1, spring constant 0.57 N m^{-1}, Olympus). All AFM images were flattened using software supplied by Shimadzu without further image processing.

ATR-IR Analysis. The ATR-IR spectra of SAv immobilized on PEI films were obtained using the refractive surface of a 100 nm-thick gold-coated poly(ethylene terephthalate) substrate (Tanaka Precious Metals) with a Spectrum One apparatus (Perkin-Elmer) in air at ambient temperature. The interferograms were co-added 50 times, and were Fourier transformed at a resolution of 4 cm^{-1}.

RESULTS AND DISCUSSION

Peptide Screening against PEI Films. Peptides with an affinity for PEI films were screened by phage display technology. After four rounds of biopanning, the amino acid sequences of the 7-mer peptides displayed on phage clones were determined (Table 1). Five different sequences (c1−c5) from 16 randomly-picked phage clones were determined. The sequence of c1 appeared 10 times, and shared a high degree of homology with c2. To confirm that the selection of these phage clones was not the result of differences in their growth rates, an amplification study was performed.[48] Each clone was incubated in a bacterial culture, and was amplified for 5 h. Except for c3 and c4, other clones showed a similar growth rate to the library and wild type phages (Supporting Information Figure S2), suggesting the possibility that the phage clone specific for PEI, such as c1 (see below), was successfully selected by the biopanning process. In fact, it has been reported that c4 is unfavorably amplified during the biopanning process.[73]

Table 1. Amino Acid Sequence of Selected Phage Clones and their Amounts Bound

clone	frequency[a]	sequence[b]	amounts bound[c]/10^3 pfu
c1	10/16	**TGADLNT**	33 ± 4
c2	1/16	**TRADLNT**	35 ± 3
c3	2/16	SPQMTLS	13 ± 12
c4	2/16	HAIYPRH	14 ± 7
c5	1/16	AQSETAP	9 ± 5
Lib			5 ± 2
wild type		no displayed peptide	10 ± 6

[a] Frequencies for the same clone in all of the isolated clones after 4 rounds of biopanning. [b] Bold: sequence homology. [c] Estimated by phage binding analysis. For all samples n = 3. The error bars represent the standard deviation.

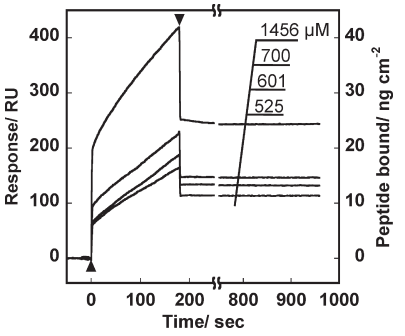

Figure 2. SPR sensorgrams of p1 for PEI films at various concentrations. ▲ and ▼ indicate the points at which the injection of the p1 solution started and ended, respectively.

The amount of each phage clone bound was investigated by phage binding analysis. The amount of c1 and c2 phage clones bound to PEI pellets was more than six-fold greater than that of the original library and was three-fold greater than that of the wild type phage. The c3−c5 phage clones also appeared, but the amounts bound were obviously smaller than the c1 and c2 phage clones. Thus, we selected the sequences of c1 and c2 to analyze the binding affinities in detail using chemically-synthesized 7-mer peptides. The chemically synthesized peptides of the c1 and c2 sequences were named p1 and p2, respectively.

Affinities of Chemically-Synthesized Peptides. The affinities of p1 and p2 for PEI films were successfully detected by highly sensitive SPR measurements. Figure 2 shows a typical example of a SPR sensorgram composed of the association and dissociation processes of p1 for the PEI films at four concentrations. The initial drastic increases in resonance units (RU) can be attributed to a change in the refractive index of the bulk solution, and are not due to p1 association. Next, a gradual RU increase, which could be quantitatively attributed to a p1 association, was observed. The subsequent replacement of the p1 solution by the buffer resulted in a drastic RU decrease, which was also the result of a refractive index change, and thus adequate amount of p1 remained. It was obvious that the amounts of p1 bound to the PEI films at a given time point increased with increasing p1 concentration, which simply reflects the fact that mass transfer to a surface is dependent on solution concentration.

The kinetic parameters and the K_a values of p1 and p2 are summarized in Table 2. The K_a of p1 for the PEI films was estimated

Table 2. Kinetic Parameters of the Peptides for the PEI Films

peptide	sequence	$k_1/M^{-1}\,s^{-1}$	k_{-1}/s^{-1}	K_a/M^{-1}
p1	TGADLNT	3.8	6.8×10^{-9}	5.6×10^{8}
		(14)[a]	(3.1×10^{-4})[a]	(4.4×10^{4})[a]
		(19)[b]	(1.5×10^{-4})[b]	(1.2×10^{5})[b]
s-p1[c]	TNDTLAG	5.4	1.5×10^{-4}	3.5×10^{4}
p1-3G	TGADGGG	4.6	1.7×10^{-4}	2.8×10^{4}
3G-p1	GGGDLNT	1.7	2.3×10^{-4}	7.7×10^{3}
p2	TRADLNT	6.4	3.3×10^{-5}	2.0×10^{5}
		(7.4)[b]	(1.5×10^{-4})[b]	(4.9×10^{4})[b]

[a] For the thermally treated PEI films. [b] For the PS films. [c] Sequence of p1 was scrambled.

to be $5.6 \times 10^8\ M^{-1}$, which was much larger than that of p2 ($2.0 \times 10^5\ M^{-1}$). The k_{-1} of p1 ($6.8 \times 10^{-9}\ s^{-1}$) was extremely small, resulting in an exceptionally large K_a as compared with short peptides, which were reported as peptides that bound to other synthetic polymers[72,74] and inorganic compounds.[75,76] As compared with synthetic polymers previously used for peptide screening, the chemical structure of PEI is relatively complicated and rigid. In addition, the molecular size of a single repeating unit of PEI is relatively larger and is comparable to that of p1 (Supporting Information Figure S3). This might suggest that a p1 bound to a PEI unit with a smaller entropic loss because of the relatively rigid structure of the PEI unit, and with a larger enthalpy gain due to the multiple interactions of the p1 side chains with the functional groups of the PEI unit. The Gibbs free energy of p1 binding (−11.9 kcal/mol) calculated from the K_a using the relationship $\Delta G_{ads} = -RT \ln K_a C$ (R = molar gas constant, T = temperature, C = 1 M as the standard concentration)[76] was slightly greater than the alkanethiolate SAMs on gold.[77] Moreover, the bound peptides were stable even after washing with a 2 M NaCl solution (Supporting Information Figure S4). Thus, p1 exhibited sufficient affinity to construct p1-modified PEI surfaces in aqueous solution.

Furthermore, the K_a of p1 for the target PEI films was more than three orders of magnitude greater than that for the reference PS films ($1.2 \times 10^5\ M^{-1}$). On the other hand, the K_a of p2 for the target PEI films ($2.0 \times 10^5\ M^{-1}$) was slightly greater than that for the reference PS films ($4.9 \times 10^4\ M^{-1}$). These results indicated that p1 was a unique peptide that binds to PEI much more strongly than to PS. Both PEI and PS have benzene ring and alkyl groups, but PEI also contains ether and imide groups. In contrast, p1 does not contain aromatic amino acids which may interact strongly with the benzene ring of PEI and PS by $\pi-\pi$ interactions, but contains amino acids such as Thr, Asp, and Asn, which can form hydrogen bonds with the ether and imide groups of PEI. Thus, hydrogen bonding of theses amino acids might be essential for binding to PEI. In addition, the second amino acid Gly from N terminus of p1 might be important for suppressing dissociation and distinguishing PEI from PS, because substituting Arg for Gly greatly raised the k_{-1} value for the PEI films and decreased the peptide specificity (see p2 in Table 2).

To understand more about the binding of p1 to PEI, the affinity of p1 for thermally treated PEI films was analyzed. The thermally treated PEI films were prepared by annealing under vacuum for 24 h at 503 K, which was more than 10 K higher than the glass transition temperature (490 K) of PEI. The K_a of p1 for the thermally treated films was estimated to be $4.4 \times 10^{-4}\ M^{-1}$, which was more than four orders of magnitude smaller than that for the as-prepared PEI films (the target in this study). Since the peptide and the polymer used in this experiment were the same, the aforementioned difference in the K_a values must be attributed to the structural difference in the PEI surfaces before and after thermal treatment. It has been reported that the degree of molecular aggregation or stacking of PEI segments is strongly influenced by the thermal history.[78] In addition, PEI was simulated to be energetically stable when the two heterocyclic imide groups were partially aligned parallel to each other.[79] Therefore, the thermal treatment is considered to induce aggregation of PEI segments at the film surface. In fact, fluorescence spectra of the thermally nontreated and treated PEI films supported the aggregation of PEI after thermal treatment (Supporting Information Figure S5). The strong fluorescence emission of the PEI films recorded after excitation at 350 nm can be interpreted as charge transfer interactions of intermolecular segments.[80] After thermal treatment, a red shift of the emission was observed, suggesting the greater aggregation state of the PEI chains. Therefore, the smaller K_a of p1 for the thermally treated PEI films might be attributed to less accessibility of p1 to PEI segments due to aggregation of PEI segments.

Table 3. Kinetic Parameters of the Biotinylated p1 for the PEI Films

peptide	$k_1/M^{-1}\,s^{-1}$	k_{-1}/s^{-1}	K_a/M^{-1}
p1-B[a]	57	3.6×10^{-4}	1.6×10^{5}
B-p1[b]	3.2	3.5×10^{-4}	9.1×10^{3}

[a] C terminus of p1 was biotinylated. [b] N terminus of p1 was biotinylated.

It is important to determine the essential part of the peptide for binding in order to conjugate with foreign molecules without losing its original binding affinity.[71] Three p1 derivatives named s-p1, 3G-p1, and p1-3G were synthesized and analyzed in the same manner to reveal which terminus of p1 is more important for binding (Table 2). s-p1 represents peptide that the primary sequence of p1 has been shuffled. 3G-p1 and p1-3G represent peptides that three amino acids from the N and C termini of p1 substituted by Gly, respectively. The shuffling of p1 sequence greatly raised the k_{-1} value (see s-p1 in Table 2), resulting in a K_a four orders of magnitude smaller than the original p1. Since the amino acid components of both peptides were the same, the importance of the primary sequence was clearly highlighted. The Gly substitution of p1 sequence also raised the k_{-1} value (see p1-3G and 3G-p1 in Table 2), indicating a strong contribution of each amino acid for binding. However, the amino acid near the N terminus of p1 might be relatively important, because the K_a of p1-3G ($2.8 \times 10^4\ M^{-1}$) was slightly larger than that of 3G-p1 ($7.7 \times 10^3\ M^{-1}$). Further experiments on biotinylated peptides supported the importance of the N terminus of p1.

The C and N termini of p1 were biotinylated (named p1-B and B-p1), respectively, and the K_as of these peptides to the PEI films were similarly estimated to be $1.6 \times 10^5\ M^{-1}$ and $9.1 \times 10^3\ M^{-1}$, respectively (Table 3). Unfortunately, the k_{-1} values of both biotinylated peptides were greatly increased by biotinylation, and therefore, the K_a values decreased as compared with that of p1. Since each amino acid of p1 was found to be essential for binding to the PEI films with an extremely high K_a as discussed above, introducing a biotin moiety and a spacer, which would not contribute to the binding, might interfere and weaken the interaction between the peptide and the PEI films. On the other

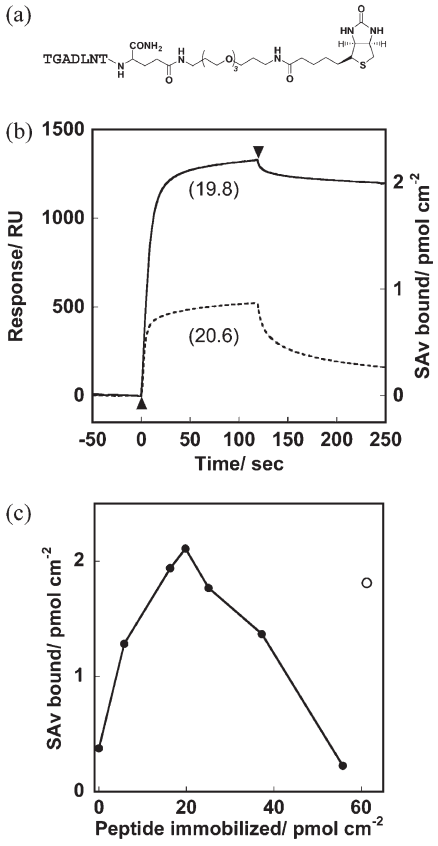

Figure 3. (a) Chemical structure of p1-B. (b) Typical SPR sensorgrams for the binding of SAv (250 nM) to $PEI_{p1\text{-}B}$ (solid line) and PEI_{p1} (dashed line) films. The parentheses indicates the amount of immobilized peptide (pmol cm^{-2}) before applying the SAv solution. ▲ and ▼ indicate the points at which the injection of SAv solution started and ended, respectively. (c) The amount of SAv bound on $PEI_{p1\text{-}B}$ films at various peptide densities (closed circle). Open circle: p1-B was immobilized together with p1 (the amounts of p1-B and p1 were assumed to be 61.2 pmol cm^{-2} and 177.7 pmol cm^{-2}, respectively, considering each peptide concentration of mixture solution).

hand, the binding constant of p1-B was greater than that of B-p1, implying that the C terminal modification was better for binding to the PEI films. In other words, the N terminal biotinylation strongly interfered with the original affinity of p1, because the N terminus of p1 is more important for binding, as discussed above. Although the biotinylation of p1 greatly affected the original affinity, the appropriate terminus for biotinylation minimized the influence. These results are consistent with a previous study which reported that the opposite terminus of the binding motif was suitable for conjugating foreign molecules to maintain the original affinity of the peptide.[71]

Immobilization of SAv via p1-B on PEI Films. On the basis of the observation that the C terminus of p1 is more suitable for conjugating a biotin moiety, p1-B (Figure 3a) was immobilized onto PEI films to further immobilize SAv (the p1-B-immobilized PEI films was named $PEI_{p1\text{-}B}$ and the other conditions were named similarly). For better accessibility of the SAv to the biotin moieties at the PEI surfaces, a biotinylated peptide was designed to have a glutamine and an ethylene glycol spacer between p1 and the biotin moiety, which resembles typical compounds used in biotin terminated-SAMs of alkanethiolates on gold.[24−29]

Figure 3b shows typical examples of SPR sensorgrams obtained when SAv bound onto $PEI_{p1\text{-}B}$ films. The amount of SAv bound was regarded as the difference in the RU between the baseline and 120 sec after buffer exchange. The RU value was converted to peptide density (pmol cm^{-2}), assuming that a SPR angle shift of 1° (= 10000 RU) corresponds to ~1 μg cm^{-2}, as previously reported.[81] The larger increase in the amount of SAv bound onto the $PEI_{p1\text{-}B}$ films (2.1 pmol cm^{-2}) as compared to SAv absorbed onto the PEI_{p1} films (0.3 pmol cm^{-2}) suggested that the SAv was mainly immobilized via p1-B. The concentration of SAv was optimized at 250 nM. When using a lower concentration (50 nM), the amount of SAv bound on the $PEI_{p1\text{-}B}$ films was smaller, indicating that some biotin moieties which could bind to SAv were left unbound. When using a higher concentration (500 nM), the amount of SAv bound on the $PEI_{p1\text{-}B}$ films was almost saturated, and a larger amount of nonspecific adsorption was observed (Supporting Information Figure S6). Thus, 250 nM SAv seemed suitable to immobilize SAv by biotin-SAv specific interactions with small amount of nonspecific adsorption.

Effects of Peptide Density at the PEI Surface on the Immobilization of SAv. Figure 3c (closed circles) shows the amount of SAv immobilized onto PEI films at various p1-B densities. The amount of SAv bound was dependent on the density of the immobilized p1-B, and showed a bell-shaped profile. Initially, the amount of SAv bound increased gradually with increasing density, and achieved a maximum (2.1 pmol cm^{-2}) at a peptide density of 19.8 pmol cm^{-2}. In fact, only 11 % of the immobilized p1-B was used for SAv binding at the maximum, when one assumed that a SAv molecule bound to a single molecule of p1-B. This percentage suggests that there are still enough biotin molecules for the binding of SAv, but that they did not work for several reasons: (i) some of the p1-B might be in an orientation that was less accessible to bind with SAv, (ii) a clustering of some of the biotin moieties might hinder the binding of SAv (see next paragraph), or (iii) some of the p1-B might be embedded inside the water swollen layer of the PEI surface (see the characterization of PEI films). It is likely that a combination of these three factors is responsible for the unavailability of some of the biotin moieties.

Moreover, the amount of SAv bound at a higher p1-B density gradually decreased. Similar trends were also reported when using biotin-terminated SAMs on gold.[27−29] It was concluded that the binding of SAv was sterically hindered on the monolayer of biotin terminated-SAMs of alkanethiolates and that the dilution of the biotinylated thiol is required to obtain good SAv binding. Unfortunately, it was difficult to visualize the peptide clustering by AFM possibly because p1-B is partially embedded in the PEI films. However, when the same amount of immobilized p1-B was spaced by p1, it resulted in an increase in the amount of SAv bound (Figure 3c, open circles), supporting the clustering of p1-B. In fact, it has been reported that gold-binding peptides also formed nuclei when bound on a gold surface.[42]

On the other hand, the surface coverage of p1-B and SAv was estimated by considering their molecular dimensions and assuming their contact faces. The p1 moiety of p1-B was assumed to bind to the PEI films with a contact area of 1.0 × 2.0 nm^2, as determined by molecular mechanic (MM2) simulation (ChemBio3D Ultra, version 11.0, CambridgeSoft) starting from the extended chain conformation, and the two biotin-binding pockets of SAv were assumed to face the PEI films with a contact area of 4.2 × 5.6 nm^2.[82] As a result, the coverage of SAv reached a maximum (30 %), when the coverage of p1-B at a peptide density

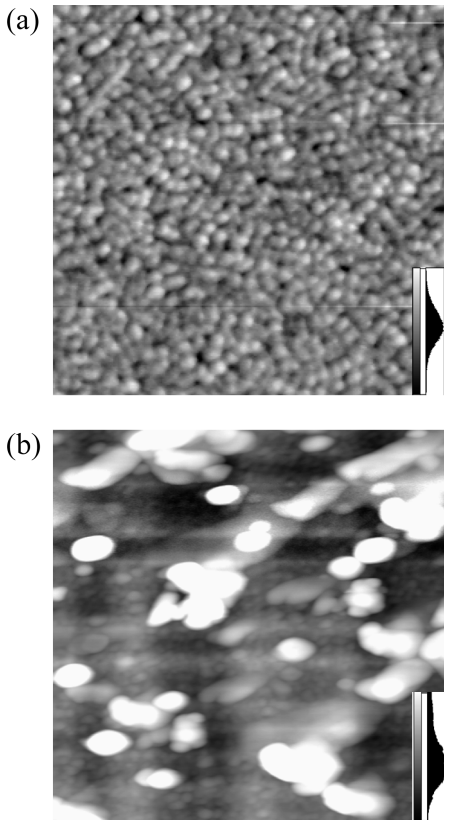

Figure 4. AFM images of SAv (a) immobilized onto PEI films via p1-B and (b) physically adsorbed onto PEI films (10 μM, 5 min). Image size: 1 μm × 1 μm. Z-scale: 4 nm.

of 19.8 pmol cm^2 was 24 %, suggesting that both the p1-B and the SAv were immobilized as monolayers.

The PEI films were characterized by measuring their film thickness and contact angle to explore the possibility that peptides might be embedded inside the water swollen layer of the PEI surface. The thickness of the PEI films was measured directly in air and in buffer. Supporting Information Figure S7 shows topographic images of the PEI films scratched by a cantilever. As a result, the thickness of the PEI films after 4 h of conditioning (10.5 ± 0.3 nm) became obviously thicker than that measured in air (9.0 ± 0.1 nm), suggesting that the PEI films swelled with buffer. In addition, the static contact angles of the PEI films measured in water using air bubble increased from 100.7 ± 1.1° to 109.8 ± 0.7° after 4 h of conditioning, indicating that the film surfaces became more hydrophilic, possibly because of water swelling. Furthermore, the angle of the PEI films after p1-B immobilization (1 mM, 30 min) remained constant. Therefore, the surface-immobilized p1-B might be partially embedded inside the water swollen layer of the PEI surface.

Characterization of Immobilized SAv. It is important to characterize the immobilized SAv to investigate the immobilization of biomolecules and to further study molecular recognition at the surfaces. AFM was used to visualize the SAv immobilized onto the PEI film via p1-B, as well as the SAv physically adsorbed onto the PEI films as references (Figure 4). Note that the amount of SAv immobilized was controlled to be approximately the same as the peak value by controlling the amount of immobilized peptide, and that a higher concentration of SAv (10 μM) was needed to physically adsorb the SAv onto the PEI films. AFM

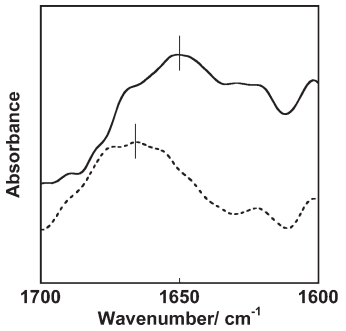

Figure 5. ATR-IR spectra of the SAv immobilized onto PEI films via p1-B (solid line) and SAv physically adsorbed onto PEI films (10 μM, 5 min, dashed line). The peak values were 1652.8 ± 0.4 and 1666.5 ± 0.1, respectively. The error bars represent the standard deviation.

images of the PEI films before and after p1-B immobilization showed little change (Supporting Information Figure S8), but after SAv immobilization, dot-like patterns were observed which were interpreted to be SAv molecules. The AFM images suggested that the SAv immobilized via p1-B was uniformly distributed as monolayer, although the physically adsorbed SAv was aggregated on the PEI films.

Structural analysis of the SAv was performed by ATR-IR, following a previous study[83] (Figure 5). ATR-IR spectra at the amide I band (1600-1700 cm^{-1}) are often used to analyze the denaturation of proteins, since it is sensitive to their secondary structures. The peak wavenumber of SAv immobilized onto the PEI films via p1-B was observed at 1652.8 ± 0.4 cm^{-1}, which is lower than that of SAv physically adsorbed onto the PEI films (1665.5 ± 0.1 cm^{-1}). A previous study suggests that the amide I band shifts to a relatively higher wavenumber with increasing random-coil content.[84,85] Accordingly, the aforementioned observations suggest that the SAv physically adsorbed onto the PEI films are relatively denatured as compared with SAv immobilized onto the PEI films via p1-B. Thus, the suppression of denaturation might be attributed to the stepwise immobilization of SAv by using the peptide.

DNA Hybridization on PEI Films. The applications of SAv immobilized onto PEI films to further immobilize a probe DNA and to observe the subsequent hybridization with the target DNA were demonstrated. Supporting Information Figure S9 shows a SPR sensorgram of the sequential binding of SAv (250 nM, 2 min), probe DNA (1 μM, 2 min), and target DNA (1 μM, 5 min) on the PEI_{p1-B} films. The binding of probe DNA and the subsequent hybridization were detected as RU increases. The saturated amount of probe DNA bound and the target DNA hybridized was estimated as the difference in the RU value between the baseline before injection and the RU value after buffer exchange (Table 4). The ratio of the amount of bound probe DNA molecules to the amount of immobilized SAv molecules was calculated at 1.5, suggesting that one molecule of SAv immobilized 1.5 molecules of the probe DNA on average. This indicated that 77% of the biotin sites were used, assuming that the two biotin sites per molecule were available. Moreover, the hybridization efficiency calculated as the ratio of the amount of hybridized target DNA to the amount of immobilized probe DNA was 95 %. Thus, it was demonstrated that the SAv immobilized onto the PEI films via p1-B maintained its biotin binding properties, and could be used for observing DNA hybridization. Unfortunately, the immobilization of probe DNA onto SAv on the PEI films was difficult to determine,

Table 4. Summary of DNA Hybridization Experiments

p1-B/pmol cm^{-2} (Γ^a/%)	SAv/pmol cm^{-2} (Γ^a/%)	probe DNA/pmol cm^{-2} (probe DNA/SAv ratio)	target DNA/pmol cm^{-2} (hybridized ratio^b/%)
11.9 ± 2.4	1.4 ± 0.1	2.1 ± 0.2	2.0 ± 0.2
(14)	(19)	(1.5)	(95)
no peptide	2.4^c	n.d.^{d}	
	(34)		

^{a} Coverage of p1-B and SAv. ^{b} Hybridized ratio was calculated as the ratio of the amount of hybridized target DNA to the amount of immobilized probe DNA. ^{c} Concentration was 10 μM. ^{d} Not determined.

because a large dissociation of the SAv was observed at the same time, suggesting that the probe DNA promoted the dissociation of denatured SAv. Previous work suggests that an uniform and well-ordered SAv film provides a well-controlled biotinylated DNA assembly, which allows for high efficiency in target DNA hybridization.[86] Thus, the aforementioned results imply that the SAv immobilized onto the PEI films via p1-B forms a well-ordered monolayer, and may be useful to probe DNA assemblies and hybridization assays.

CONCLUSIONS

We demonstrated the selection and characterization of PEI-binding peptides, and their application as surface modifiers. Peptides that bind specifically to PEI films were successfully identified from a phage-displayed peptide library. SPR analysis revealed that the chemically-synthesized 7-mer peptide p1 (Thr-Gly-Ala-Asp-Leu-Asn-Thr) had an extremely high binding constant for the PEI films (5.6×10^8 M^{-1}), which was more than three orders of magnitude greater than for the reference PS films. p1 was biotinylated and immobilized onto the PEI films to further immobilize SAv. We found that several factors could significantly affect the amount of SAv bound. It gradually increased with an increasing density of immobilized p1-B, and the appropriate density allowed for the maximum amount of SAv bound. Most of the p1-B immobilized onto the PEI surface showed low accessibility to bind with SAv. In addition, some of the p1-B was suggested to be clustered, which resulted in a decrease of the amount of SAv bound at high peptide density. Furthermore, we demonstrated that the SAv immobilized via p1-B onto the PEI films was uniformly distributed, and thus was able to further immobilize probe DNA in order to observe hybridization with complementary DNA. This is the first report identifying and characterizing a PEI-binding peptide, and demonstrated its potential as a surface modifier. The present study offered new and significant insights into the modification of polymer surfaces using MBPs. This could potentially lead to new techniques of analyzing the molecular recognition of biomolecules on various material surfaces.

ASSOCIATED CONTENT

Supporting Information. Explanation of baseline corrections of SPR sensorgrams, the fitting results including the chi-square values and the standard errors, a chemical structure of biotinylation regent, phage amplification experiments, illustrations of p1 and a single unit of PEI, binding stability of p1, fluorescence spectra of PEI films, amount of SAv immobilized onto PEI films for different concentrations of SAv, thickness measurements of PEI films, AFM images of PEI films before and after p1-B immobilization, and SPR sensorgrams of DNA hybridization experiments (PDF). This material is available free of charge via the Internet at http://pubs.acs.org.

AUTHOR INFORMATION

Corresponding Author

*Phone: +81-3-5452-5224. E-mail: t-serizawa@bionano.rcast.u-tokyo.ac.jp.

Present Addresses

[⊥]Yu Initiative Research Unit, RIKEN Advanced Science Institute.
[¶]Department of Applied Chemistry, Kyushu University.

ACKNOWLEDGMENT

Authors thank Prof. H. Aburatani (The University of Tokyo) for DNA sequencing and Prof. M. Komiyama (The University of Tokyo) for MALDI TOF-MS measurements. T.D. is grateful to the Japan Society for the Promotion of Science (JSPS) for a Research Fellow Ship for Young Scientists. This study was financially supported in part by Fuji Electric Holdings and the Ministry of Education, Culture, Sports, Science and Technology of Japan (Grants-in-Aid for Scientific Research (B) no. 20350052 to T.S., Grants-in-Aid for New Academic Field Research no. 21106506 to T.S., and Global COE program "Chemistry Innovation through Cooperation of Science and Engineering").

REFERENCES

(1) Ulman, A. *Chem. Rev.* **1996**, *96*, 1533–1554.
(2) Onclin, S.; Ravoo, B. J.; Reinhoudt, D. N. *Angew. Chem., Int. Ed.* **2005**, *44*, 6282–6304.
(3) Love, J. C.; Estroff, L. A.; Kriebel, J. K.; Nuzzo, R. G.; Whitesides, G. M. *Chem. Rev.* **2005**, *105*, 1103–1169.
(4) Allara, D. L.; Nuzzo, R. G. *Langmuir* **1985**, *1*, 45–52.
(5) Allara, D. L.; Nuzzo, R. G. *Langmuir* **1985**, *1*, 52–66.
(6) Sagiv, J. *J. Am. Chem. Soc.* **1980**, *102*, 92–98.
(7) Nuzzo, R. G.; Allara, D. L. *J. Am. Chem. Soc.* **1983**, *105*, 4481–4483.
(8) Sheen, C. W.; Shi, J. X.; Martensson, J.; Parikh, A. N.; Allara, D. L. *J. Am. Chem. Soc.* **1992**, *114*, 1514–1515.
(9) Linford, M. R.; Chidsey, C. E. D. *J. Am. Chem. Soc.* **1993**, *115*, 12631–12632.
(10) Herne, T. M.; Tarlov, M. J. *J. Am. Chem. Soc.* **1997**, *119*, 8916–8920.
(11) Peterlinz, K. A.; Georgiadis, R. M.; Herne, T. M.; Tarlov, M. J. *J. Am. Chem. Soc.* **1997**, *119*, 3401–3402.
(12) ODonnell, M. J.; Tang, K.; Koster, H.; Smith, C. L.; Cantor, C. R. *Anal. Chem.* **1997**, *69*, 2438–2443.
(13) Strother, T.; Cai, W.; Zhao, X. S.; Hamers, R. J.; Smith, L. M. *J. Am. Chem. Soc.* **2000**, *122*, 1205–1209.
(14) Pilloud, D. L.; Rabanal, F.; Gibney, B. R.; Farid, R. S.; Dutton, P. L.; Moser, C. C. *J. Phys. Chem. B* **1998**, *102*, 1926–1937.

(15) MacBeath, G.; Schreiber, S. L. *Science* **2000**, *289*, 1760–1763.
(16) Wegner, G. J.; Lee, H. J.; Corn, R. M. *Anal. Chem.* **2002**, *74*, 5161–5168.
(17) Watzke, A.; Kohn, M.; Gutierrez-Rodriguez, M.; Wacker, R.; Schroder, H.; Breinbauer, R.; Kuhlmann, J.; Alexandrov, K.; Niemeyer, C. M.; Goody, R. S.; Waldmann, H. *Angew. Chem., Int. Ed.* **2006**, *45*, 1408–1412.
(18) Inamori, K.; Kyo, M.; Matsukawa, K.; Inoue, Y.; Sonoda, T.; Tatematsu, K.; Tanizawa, K.; Mori, T.; Katayama, Y. *Anal. Chem.* **2008**, *80*, 643–650.
(19) Rogero, C.; Chaffey, B. T.; Mateo-Marti, E.; Sobrado, J. M.; Horrocks, B. R.; Houlton, A.; Lakey, J. H.; Briones, C.; Martin-Gago, J. A. *J. Phys. Chem. C* **2008**, *112*, 9308–9314.
(20) Horan, N.; Yan, L.; Isobe, H.; Whitesides, G. M.; Kahne, D. *Proc. Natl. Acad. Sci. U. S. A.* **1999**, *96*, 11782–11786.
(21) Smith, E. A.; Thomas, W. D.; Kiessling, L. L.; Corn, R. M. *J. Am. Chem. Soc.* **2003**, *125*, 6140–6148.
(22) Blixt, O.; Head, S.; Mondala, T.; Scanlan, C.; Huflejt, M. E.; Alvarez, R.; Bryan, M. C.; Fazio, F.; Calarese, D.; Stevens, J.; Razi, N.; Stevens, D. J.; Skehel, J. J.; van Die, I.; Burton, D. R.; Wilson, I. A.; Cummings, R.; Bovin, N.; Wong, C. H.; Paulson, J. C. *Proc. Natl. Acad. Sci. U. S. A.* **2004**, *101*, 17033–17038.
(23) Park, S.; Lee, M. R.; Pyo, S. J.; Shin, I. *J. Am. Chem. Soc.* **2004**, *126*, 4812–4819.
(24) Haussling, L.; Ringsdorf, H.; Schmitt, F. J.; Knoll, W. *Langmuir* **1991**, *7*, 1837–1840.
(25) Haussling, L.; Michel, B.; Ringsdorf, H.; Rohrer, H. *Angew. Chem., Int. Ed.* **1991**, *30*, 569–572.
(26) Muller, W.; Ringsdorf, H.; Rump, E.; Wildburg, G.; Zhang, X.; Angermaier, L.; Knoll, W.; Liley, M.; Spinke, J. *Science* **1993**, *262*, 1706–1708.
(27) Spinke, J.; Liley, M.; Schmitt, F. J.; Guder, H. J.; Angermaier, L.; Knoll, W. *J. Chem. Phys.* **1993**, *99*, 7012–7019.
(28) Spinke, J.; Liley, M.; Guder, H. J.; Angermaier, L.; Knoll, W. *Langmuir* **1993**, *9*, 1821–1825.
(29) Perez-Luna, V. H.; O'Brien, M. J.; Opperman, K. A.; Hampton, P. D.; Lopez, G. P.; Klumb, L. A.; Stayton, P. S. *J. Am. Chem. Soc.* **1999**, *121*, 6469–6478.
(30) Sarikaya, M.; Tamerler, C.; Jen, A. K. Y.; Schulten, K.; Baneyx, F. *Nat. Mater.* **2003**, *2*, 577–585.
(31) Patwardhan, S. V.; Patwardhan, G.; Perry, C. C. *J. Mater. Chem.* **2007**, *17*, 2875–2884.
(32) Baneyx, F.; Schwartz, D. T. *Curr. Opin. Biotechnol.* **2007**, *18*, 312–317.
(33) Dickerson, M. B.; Sandhage, K. H.; Naik, R. R. *Chem. Rev.* **2008**, *108*, 4935–4978.
(34) Whaley, S. R.; English, D. S.; Hu, E. L.; Barbara, P. F.; Belcher, A. M. *Nature* **2000**, *405*, 665–668.
(35) Sano, K. I.; Shiba, K. *J. Am. Chem. Soc.* **2003**, *125*, 14234–14235.
(36) Braun, R.; Sarikaya, M.; Schulten, K. *J. Biomater. Sci. Polym. Ed.* **2002**, *13*, 747–757.
(37) Oren, E. E.; Tamerler, C.; Sarikaya, M. *Nano Lett.* **2005**, *5*, 415–419.
(38) Serizawa, T.; Sawada, T.; Matsuno, H.; Matsubara, T.; Sato, T. *J. Am. Chem. Soc.* **2005**, *127*, 13780–13781.
(39) Serizawa, T.; Sawada, T.; Kitayama, T. *Angew. Chem., Int. Ed.* **2007**, *46*, 723–726.
(40) Heinz, H.; Farmer, B. L.; Pandey, R. B.; Slocik, J. M.; Patnaik, S. S.; Pachter, R.; Naik, R. R. *J. Am. Chem. Soc.* **2009**, *131*, 9704–9714.
(41) Sawada, T.; Takahashi, T.; Mihara, H. *J. Am. Chem. Soc.* **2009**, *131*, 14434–14441.
(42) So, C. R.; Tamerler, C.; Sarikaya, M. *Angew. Chem., Int. Ed.* **2009**, *48*, 5174–5177.
(43) Sano, K.; Ajima, K.; Iwahori, K.; Yudasaka, M.; Iijima, S.; Yamashita, I.; Shiba, K. *Small* **2005**, *1*, 826–832.
(44) Park, T. J.; Lee, S. Y.; Lee, S. J.; Park, J. P.; Yang, K. S.; Lee, K. B.; Ko, S.; Park, J. B.; Kim, T.; Kim, S. K.; Shin, Y. B.; Chung, B. H.; Ku, S. J.; Kim, D. H.; Choi, I. S. *Anal. Chem.* **2006**, *78*, 7197–7205.
(45) Matsui, T.; Matsukawa, N.; Iwahori, K.; Sano, K. I.; Shiba, K.; Yamashita, I. *Langmuir* **2007**, *23*, 1615–1618.
(46) Kashiwagi, K.; Tsuji, T.; Shiba, K. *Biomaterials* **2009**, *30*, 1166–1175.
(47) Kacar, T.; Zin, M. T.; So, C.; Wilson, B.; Ma, H.; Gul-Karaguler, N.; Jen, A. K. Y.; Sarikaya, M.; Tamerler, C. *Biotechnol. Bioeng.* **2009**, *103*, 696–705.
(48) Sanghvi, A. B.; Miller, K. P. H.; Belcher, A. M.; Schmidt, C. E. *Nat. Mater.* **2005**, *4*, 496–502.
(49) Meyers, S. R.; Hamilton, P. T.; Walsh, E. B.; Kenan, D. J.; Grinstaff, M. W. *Adv. Mater.* **2007**, *19*, 2492–2498.
(50) Meyers, S. R.; Khoo, X. J.; Huang, X.; Walsh, E. B.; Grinstaff, M. W.; Kenan, D. J. *Biomaterials* **2009**, *30*, 277–286.
(51) Tamerler, C.; Duman, M.; Oren, E. E.; Gungormus, M.; Xiong, X. R.; Kacar, T.; Parviz, B. A.; Sarikaya, M. *Small* **2006**, *2*, 1372–1378.
(52) Kacar, T.; Ray, J.; Gungormus, M.; Oren, E. E.; Tamerler, C.; Sarikaya, M. *Adv. Mater.* **2009**, *21*, 295–299.
(53) Serizawa, T.; Hirai, Y.; Aizawa, M. *Langmuir* **2009**, *25*, 12229–12234.
(54) Kenan, D. J.; Walsh, E. B.; Meyers, S. R.; O'Toole, G. A.; Carruthers, E. G.; Lee, W. K.; Zauscher, S.; Prata, C. A.; Grinstaff, M. W. *Chem. Biol.* **2006**, *13*, 695–700.
(55) Khoo, X.; Hamilton, P.; O'Toole, G. A.; Snyder, B. D.; Kenan, D. J.; Grinstaff, M. W. *J. Am. Chem. Soc.* **2009**, *131*, 10992–10997.
(56) Kurtz, S. M.; Devine, J. N. *Biomaterials* **2007**, *28*, 4845–4869.
(57) Imai, Y.; Watanabe, A.; Masuhara, E.; Imai, Y. *J. Biomed. Mater. Res.* **1983**, *17*, 905–912.
(58) Wenz, L. M.; Merritt, K.; Brown, S. A.; Moet, A.; Steffee, A. D. *J. Biomed. Mater. Res.* **1990**, *24*, 207–215.
(59) Richardson, R. R., Jr.; Miller, J. A.; Reichert, W. M. *Biomaterials* **1993**, *14*, 627–635.
(60) Morrison, C.; Macnair, R.; MacDonald, C.; Wykman, A.; Goldie, I.; Grant, M. H. *Biomaterials* **1995**, *16*, 987–992.
(61) Petillo, O.; Peluso, G.; Ambrosio, L.; Nicolais, L.; Kao, W. J.; Anderson, J. M. *J. Biomed. Mater. Res.* **1994**, *28*, 635–646.
(62) Peluso, G.; Petillo, O.; Ambrosio, L.; Nicolais, L. *J. Mater. Sci.: Mater. Med.* **1994**, *5*, 738–742.
(63) Noiset, O.; Schneider, Y. J.; Marchand-Brynaert, J. *J. Biomater. Sci. Polym. Ed.* **1999**, *10*, 657–677.
(64) Noiset, O.; Schneider, Y. J.; Marchand-Brynaert, J. *J. Biomater. Sci. Polym. Ed.* **2000**, *11*, 767–786.
(65) Albrecht, W.; Seifert, B.; Weigel, T.; Schossig, M.; Hollander, A.; Groth, T.; Hilke, R. *Macromol. Chem. Phys.* **2003**, *204*, 510–521.
(66) Santoso, F.; Albrecht, W.; Schroeter, M.; Weigel, T.; Paul, D.; Schomacker, R. *J. Membr. Sci.* **2003**, *223*, 171–185.
(67) Albrecht, W.; Santoso, F.; Lutzow, K.; Weigel, T.; Schomacker, R.; Lendlein, A. *J. Membr. Sci.* **2007**, *292*, 145–157.
(68) Briem, D.; Strametz, S.; Schroder, K.; Meenen, N. M.; Lehmann, W.; Linhart, W.; Ohl, A.; Rueger, J. M. *J. Mater. Sci. Mater. Med.* **2005**, *16*, 671–677.
(69) Kaba, M.; Essamri, A.; Mas, A.; Schue, F.; George, G. A.; Cardona, F.; Rintoul, L.; Wood, B. J. *J. Appl. Polym. Sci.* **2006**, *100*, 3579–3588.
(70) D'Britto, V.; Tiwari, S.; Purohit, V.; Wadgaonkar, P. P.; Bhoraskar, S. V.; Bhonde, R. R.; Prasad, B. L. V. *J. Mater. Chem* **2009**, *19*, 544–550.
(71) Date, T.; Tanaka, K.; Nagamura, T.; Serizawa, T. *Chem. Mater.* **2008**, *20*, 4536–4538.
(72) Serizawa, T.; Sawada, T.; Matsuno, H. *Langmuir* **2007**, *23*, 11127–11133.
(73) Brammer, L. A.; Bolduc, B.; Kass, J. L.; Felice, K. M.; Noren, C. J.; Hall, M. F. *Anal. Biochem.* **2008**, *373*, 88–98.
(74) Matsuno, H.; Sekine, J.; Yajima, H.; Serizawa, T. *Langmuir* **2008**, *24*, 6399–6403.

(75) Sano, K. I.; Sasaki, H.; Shiba, K. *Langmuir* **2005**, *21*, 3090–3095.
(76) Tamerler, C.; Oren, E. E.; Duman, M.; Venkatasubramanian, E.; Sarikaya, M. *Langmuir* **2006**, *22*, 7712–7718.
(77) Karpovich, D. S.; Blanchard, G. J. *Langmuir* **1994**, *10*, 3315–3322.
(78) Hasegawa, M.; Kochi, M.; Mita, I.; Yokota, R. *Eur. Polym. J.* **1989**, *25*, 349–354.
(79) Xia, J.; Liu, S.; Pallathadka, P. K.; Chng, M. L.; Chung, T.-S. *Ind. Eng. Chem. Res.* **2010**, *49*, 12014–12021.
(80) Viallat, A.; Bom, R. P.; Cohenaddad, J. P. *Polymer* **1994**, *35*, 2730–2736.
(81) Stenberg, E.; Persson, B.; Roos, H.; Urbaniczky, C. *J. Colloid Interface Sci.* **1991**, *143*, 513–526.
(82) Weber, P. C.; Ohlendorf, D. H.; Wendoloski, J. J.; Salemme, F. R. *Science* **1989**, *243*, 85–88.
(83) Jackson, M.; Mantsch, H. H. *Rev. Biochem. Mol. Biol.* **1995**, *30*, 95–120.
(84) Fernandez-Ballester, G.; Castresana, J.; Arrondo, J. L.; Ferragut, J. A.; Gonzalez-Ros, J. M. *Biochem. J.* **1992**, *288*, 421–426.
(85) Hernandez-Perez, M. A.; Garapon, C.; Champeaux, C.; Shahgaldian, P.; Coleman, A.; Mugnier, J. *Appl. Surf. Sci.* **2003**, *208*, 658–662.
(86) Su, X. D.; Wu, Y. J.; Robelek, R.; Knoll, W. *Langmuir* **2005**, *21*, 348–353.